

Exact nonlinear fourth-order equation for two coupled nonlinear oscillators: metamorphoses of resonance curves

Jan Kyzioł¹⁾, Andrzej Okninski²⁾

Department of Mechatronics and Mechanical Engineering¹⁾,
 Department of Management and Computer Modelling²⁾,
 Politechnika Świętokrzyska, Al. 1000-lecia PP7,
 25-314 Kielce, Poland

April 1, 2024

Abstract

We study dynamics of two coupled periodically driven oscillators. The internal motion is separated off exactly to yield a nonlinear fourth-order equation describing inner dynamics. Periodic steady-state solutions of the fourth-order equation are determined within the Krylov-Bogoliubov-Mitropolsky approach – we compute the amplitude profiles, which from mathematical point of view are algebraic curves.

In the present paper we investigate metamorphoses of amplitude profiles induced by changes of control parameters near singular points of these curves. It follows that dynamics changes qualitatively in the neighbourhood of a singular point.

1 Introduction

In this work we study dynamics of two coupled oscillators, one of which is driven by an external periodic force. Equations governing dynamics of such system are of form:

$$\left. \begin{aligned} m_1 \ddot{x}_1 - V_1(\dot{x}_1) - R_1(x_1) + V_2(\dot{x}_2 - \dot{x}_1) + R_2(x_2 - x_1) &= f \cos(\omega t) \\ m_2 \ddot{x}_2 - V_2(\dot{x}_2 - \dot{x}_1) - R_2(x_2 - x_1) &= 0 \end{aligned} \right\} \quad (1)$$

where R_1 , V_1 and R_2 , V_2 are nonlinear elastic restoring force and nonlinear force of internal friction for mass m_1 and mass m_2 , respectively. Dynamic vibration absorber, consisting of a (generally small) mass m_2 , attached to the primary vibrating system of (typically larger) mass m_1 is a generic mechanical model described by (1) [1, 2].

We shall consider a special case:

$$R_1(x_1) = -\alpha_1 x_1, \quad V_1(\dot{x}_1) = -\nu_1 \dot{x}_1. \quad (2)$$

Dynamics of coupled periodically driven oscillators is very complicated [3, 4, 5, 6, 7, 8]. Starting from equations (1), (2) we derived the exact fourth-order nonlinear equation for internal motion as well as approximate second-order effective equation [9, 10] (this approximation performs well for $\frac{m_2}{m_1} \ll 1$). Applying the Krylov-Bogoliubov-Mitropolsky (KBM) method to the effective equation we have computed and studied the corresponding nonlinear resonances. More exactly, we investigated the amplitude profiles (resonance curves) $A(\omega)$, i.e. dependence of the amplitude on the frequency ω , given implicitly by the KBM method. Metamorphoses of the resonance curves $A(\omega)$ induced by changes of the control parameters, leading to new nonlinear phenomena, have been studied within the theory of algebraic curves – they occur in the neighbourhoods of singular points of $A(\omega)$ [11, 12, 13].

In the present paper we study the exact fourth-order equation for internal motion. It turns out that the KBM method can be applied to yield equation defining the amplitude profile $A(\omega; a, b, \dots)$ implicitly, where a, b, \dots are some parameters. This resonance curve is more complicated then in the case of effective equation and hence more complicated metamorphoses are possible. The aim of the present paper is to explore these possibilities.

The paper is organized as follows. In the next Section the exact 4th-order equation for the internal motion in non-dimensional form is presented. In Section 3 equation for the resonance curves $A(\omega)$ is derived from the exact fourth-order equation for internal motion via the Krylov-Bogoliubov-Mitropolsky approach. In Section 4 the theory of algebraic curves is used to compute singular points on the exact equation amplitude profiles - metamorphoses of amplitude profiles occur in neighbourhoods of such points. In Section 5 examples of analytical and numerical computations are presented for the 4th-order equation. Our results are summarized in the last Section.

2 Exact equation for internal motion

In new variables, $x \equiv x_1$, $y \equiv x_2 - x_1$, equations (1), (2) can be written as:

$$\left. \begin{aligned} m\ddot{x} + \nu\dot{x} + \alpha x + V_e(\dot{y}) + R_e(y) &= f \cos(\omega t) \\ m_e(\ddot{x} + \ddot{y}) - V_e(\dot{y}) - R_e(y) &= 0 \end{aligned} \right\}, \quad (3)$$

where $m \equiv m_1$, $m_e \equiv m_2$, $\nu \equiv \nu_1$, $\alpha \equiv \alpha_1$, $V_e \equiv V_2$, $R_e \equiv R_2$.

Adding equations (3) we obtain important relation between variables x and y :

$$M\ddot{x} + \nu_1\dot{x} + \alpha_1 x + m_e\ddot{y} = f \cos(\omega t), \quad (4)$$

where $M = m + m_e$.

We can eliminate variable x in (3) to obtain the following exact equation for relative motion:

$$\left(M \frac{d^2}{dt^2} + \nu \frac{d}{dt} + \alpha\right) (\mu \ddot{y} - V_e(\dot{y}) - R_e(y)) + \epsilon m_e \left(\nu \frac{d}{dt} + \alpha\right) \ddot{y} = F \cos(\omega t), \quad (5)$$

where $F = m_e \omega^2 f$, $\mu = m m_e / M$ and $\epsilon = m_e / M$ is a nondimensional parameter [9, 10], see also Ref. [14] where separation of variables for a more general system of coupled equations was described. Equations (5), (4) are equivalent to the initial equations (1), (2).

For small ϵ we can reject the term proportional to ϵ to obtain the approximate (effective) equation which can be integrated partly to yield the effective equation:

$$\mu \ddot{y} - V_e(\dot{y}) - R_e(y) = \frac{-m_e \omega^2 f}{\sqrt{M^2 \left(\omega^2 - \frac{\alpha}{M}\right)^2 + \nu^2 \omega^2}} \cos(\omega t + \delta). \quad (6)$$

In what follows we shall assume

$$R_e(y) = -\alpha_e y - \gamma_e y^3, \quad V_e(\dot{y}) = -\nu_e \dot{y} + \lambda_e \dot{y}^3. \quad (7)$$

This model was also investigated in [8] where limiting phase trajectories approach was used.

In this work we shall investigate the exact equation (5). We write Eqns. (5), (7) in nondimensional form. Introducing nondimensional time τ and rescaling variable y :

$$\tau = t \bar{\omega}, \quad z = y \sqrt{\frac{\gamma_e}{\alpha_e}}, \quad (8)$$

where:

$$\bar{\omega} = \sqrt{\frac{\alpha_e}{\mu}}, \quad (9)$$

we get:

$$\hat{\mathcal{L}} \left(\frac{d^2 z}{d\tau^2} + h \frac{dz}{d\tau} - b \left(\frac{dz}{d\tau} \right)^3 + z + z^3 \right) + \kappa \left(H \frac{d}{d\tau} + a \right) \frac{d^2 z}{d\tau^2} = \frac{\kappa}{\kappa+1} G \Omega^2 \cos(\Omega \tau) \quad (10)$$

where $\hat{\mathcal{L}}$ is a linear operator:

$$\hat{\mathcal{L}} = \frac{d^2}{d\tau^2} + H \frac{d}{d\tau} + a, \quad (11)$$

and nondimensional constants are given by:

$$h = \frac{\nu_e}{\mu \bar{\omega}}, \quad b = \frac{\lambda_e}{\gamma_e} \bar{\omega}^3, \quad H = \frac{\nu}{M \bar{\omega}}, \quad \Omega = \frac{\omega}{\bar{\omega}}, \quad G = \frac{1}{\alpha_e} \sqrt{\frac{\gamma_e}{\alpha_e}} f, \quad \kappa = \frac{m_e}{m}, \quad a = \frac{\alpha \mu}{\alpha_e M}. \quad (12)$$

3 Nonlinear resonances via Krylov-Bogoliubov-Mitropolsky method

We apply the Krylov-Bogoliubov-Mitropolsky (KBM) perturbation approach [15] to the exact nonlinear fourth-order equation (10) describing internal motion of the small mass. The equation (10) is written in the following form:

$$\hat{\mathcal{L}} \left(\frac{d^2 z}{d\tau^2} + \Omega^2 z \right) + \varepsilon \left(\sigma \hat{\mathcal{L}} z + g(z, \dot{z}) \right) = 0, \quad (13)$$

where $\hat{\mathcal{L}}$ is defined in (11) and $\varepsilon g(z, \dot{z})$ is given by:

$$\varepsilon g = \hat{\mathcal{L}} \left(h \frac{dz}{d\tau} - b \left(\frac{dz}{d\tau} \right)^3 + z + z^3 \right) - \Theta^2 \hat{\mathcal{L}} z + \kappa \left(H \frac{d}{d\tau} + a \right) \frac{d^2 z}{d\tau^2} - \frac{\kappa}{\kappa+1} G \Omega^2 \cos(\Omega\tau), \quad (14)$$

and

$$\Theta^2 - \Omega^2 = \varepsilon \sigma. \quad (15)$$

Equation (13) was prepared in such way that for $\varepsilon = 0$ the general solution, $z(\tau) = A \cos(\Omega\tau + \varphi) + C \exp\left(-\frac{1}{2}(H - \sqrt{\Delta})\tau\right) + D \exp\left(-\frac{1}{2}(H + \sqrt{\Delta})\tau\right)$, $\Delta = H^2 - 4a$, with constant and arbitrary A, φ, C, D and, moreover, the solution for $H, a > 0$ does not contain secular terms and $z(\tau) \rightarrow A \cos(\Omega\tau + \varphi)$ for $\tau \rightarrow \infty$.

We shall now look for 1 : 1 resonance using the KBM method. For small nonzero ε the solution of Eqns.(13) – (15) and (7) is sought in form:

$$z = A \cos(\Omega\tau + \varphi) + \varepsilon z_1(A, \varphi, \tau) + \dots \quad (16)$$

with slowly varying amplitude and phase:

$$\frac{dA}{d\tau} = \varepsilon M_1(A, \varphi) + \dots, \quad (17)$$

$$\frac{d\varphi}{d\tau} = \varepsilon N_1(A, \varphi) + \dots \quad (18)$$

Computing now derivatives of z from Eqns.(16), (17), (18) and substituting to Eqns.(13) – (15), (7) and eliminating secular terms and demanding $M_1 = 0$, $N_1 = 0$ we obtain the following equations for the amplitude and phase of steady states:

$$-\Omega A (p\Omega^2 - q) + \frac{3}{4}\Omega A^3 (H - ba\Omega^2 + b\Omega^4) + \frac{\kappa}{\kappa+1} G \Omega^2 \sin \varphi = 0, \quad (19a)$$

$$-A (\Omega^4 - r\Omega^2 + a) - \frac{3}{4}A^3 (a - \Omega^2 + Hb\Omega^4) + \frac{\kappa}{\kappa+1} G \Omega^2 \cos \varphi = 0. \quad (19b)$$

where $p = h + H(\kappa + 1)$, $q = ah + H$, $r = hH + a(\kappa + 1) + 1$.

Solving the system of equations (19) we get the implicit expressions for the

amplitude $A(\Omega)$ and the phase $\varphi(\Omega)$:

$$A(\Omega) = \frac{\kappa G}{\kappa + 1} \frac{\Omega^2}{\sqrt{C^2 + D^2}}, \quad (20a)$$

$$\tan \varphi(\Omega) = \frac{C}{D}, \quad (20b)$$

$$C = \Omega A(\Omega) (p\Omega^2 - q) - \frac{3}{4}\Omega A^3(\Omega) (H - ba\Omega^2 + b\Omega^4) \quad (20c)$$

$$D = A(\Omega) (\Omega^4 - r\Omega^2 + a) + \frac{3}{4}A^3(\Omega) (a - \Omega^2 + Hb\Omega^4) \quad (20d)$$

Equation for the correcting term z_1 is of form:

$$\hat{\mathcal{L}} \left(\frac{d^2 z_1}{dt^2} + \Omega^2 z_1 \right) = \frac{3}{4}H\Omega A^3 \sin(\Phi) + \frac{1}{4}A^3 ((3+a)\Omega^2 - 3b) \cos(\Phi), \quad (21)$$

where $\Phi \equiv 3\Omega\tau + 3\varphi(\Omega)$. Solving Eqn.(21) and substituting to (16) we get finally:

$$z = A(\Omega) \cos(\Omega\tau + \varphi) - \frac{1}{32}A^3(\Omega) b\Omega \sin(\Phi) + \frac{1}{32\Omega^2}A^3(\Omega) \cos(\Phi) \quad (22)$$

where $A(\Omega)$, $\varphi(\Omega)$ are given by Eqns.(20).

4 General properties of the function $A(\Omega)$

After introducing new variables, $\Omega^2 = X$, $A^2 = Y$, the equation (20a) defining the amplitude profile reads

$$L(X, Y; a, b, h, H, \kappa, J) \stackrel{df}{=} XY \left(pX - q - \frac{3}{4}Y (H - abX + bX^2) \right)^2 + Y \left(X^2 - rX + a + \frac{3}{4}Y (a - X + bHX^2) \right)^2 - JX^2 = 0 \quad (23)$$

where, as before, $p = h + H(\kappa + 1)$, $q = ah + H$, $r = hH + a(\kappa + 1) + 1$. A new parameter J is a renormalized G , $J = \left(\frac{\kappa}{\kappa+1} \right)^2 G^2$. To obtain the corresponding expression for the effective equation (6) one can put $G = \gamma \frac{\kappa+1}{\kappa}$ so that $J = \gamma^2$ and then $\kappa = 0$.

Singular points of $L(X, Y)$ are computed from equations [16]:

$$L = 0, \quad (24a)$$

$$\frac{\partial L}{\partial X} = 0, \quad (24b)$$

$$\frac{\partial L}{\partial Y} = 0. \quad (24c)$$

We can eliminate J from Eqns. (24a), (24b) computing $L - \frac{1}{2}X \frac{\partial L}{\partial X} = \frac{1}{32}YK$ where

$$\begin{aligned} K = & -18b^2H^2X^4Y^2 - 24a^2(\kappa+1)XY + 24bhH^2X^3Y - 48bHX^4Y \\ & -18aXY^2 - 48aXY + 32HhX^3 + 32a^2 - 27b^2X^5Y^2 + 16H^2X \\ & -32aX - 32a^2(\kappa+1)X + 32a(\kappa+1)X^3 + 9H^2XY^2 + 24H^2XY \\ & +48a^2Y + 18a^2Y^2 + 48hbX^4Y - 9a^2b^2X^3Y^2 + 36ab^2X^4Y^2 \\ & +16a^2h^2X - 16(\kappa+1)^2H^2X^3 + 48bH(\kappa+1)X^4Y \\ & -32hH(\kappa+1)X^3 - 48abhX^3Y + 32X^3 - 16h^2X^3 - 32X^4 + 24X^3Y \end{aligned} \quad (25)$$

to obtain simplified equations:

$$K = 0, \quad (26)$$

$$\frac{\partial L}{\partial Y} = 0, \quad (27)$$

from which X , Y can be computed as functions of parameters a , b , h , H , κ and, finally, J can be computed from the last equation

$$\frac{\partial L}{\partial X} = 0. \quad (28)$$

Equations (26), (27), (28) are still very complicated making analytical investigation virtually impossible. We shall thus solve these equations numerically.

5 Computational results

In the present Section singular points of amplitude profiles – solutions of Eqs. (26), (27), (28) – are studied. More exactly, resonance curves with one singular point, two singular points on one curve, and with degenerate singular point are presented and metamorphoses of bifurcation diagrams are shown.

5.1 Amplitude profiles with one singular point

We have computed singular points for the following values of control parameters: $\kappa = 0.05$, $b = -0.001$, $H = 0.4$, $a = 5$, $h = 0.5$ obtaining four physical solutions (i.e. with $X > 0$, $Y > 0$, $J > 0$):

Table 1.			
X	Y	J	n
2.170 051 157	1.357 255 661	1.656 917 694 08	1
4.835 083 103	4.192 055 014	1.036 434 991 78	2
2.798 801 078	1.237 140 868	1.814 387 388 23	3
4.153 001 386	4.680 111 331	0.963 352 653 58	4

The first two solutions correspond to self-intersections, see Fig. 1, while the second pair represents isolated points.

Metamorphoses of bifurcation diagrams which occur in the neighbourhood of self-intersections for the exact fourth-order equation are, for small κ , qualitatively similar to those studied for the case of 1 : 1 resonance in the effective equation in [11, 13] and are not shown here.

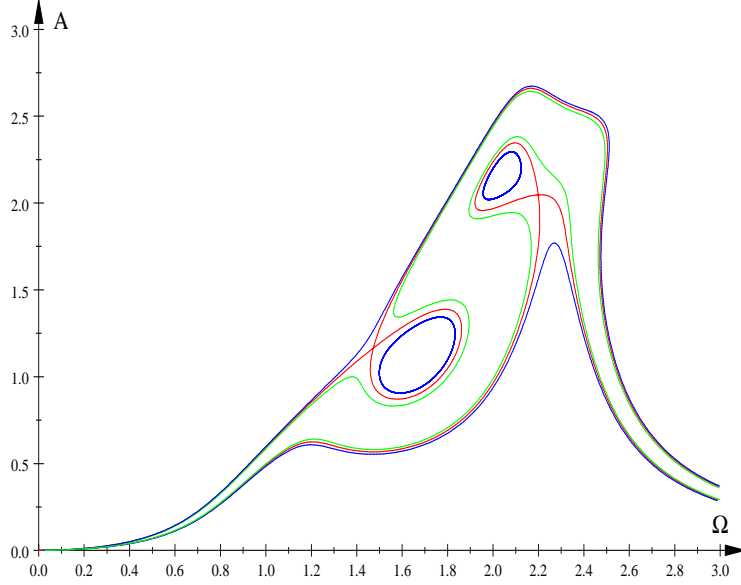


Figure 1: Amplitude profiles with singular points, $\kappa = 0.05$, $b = -0.001$, $H = 0.4$, $a = 5$, $h = 0.5$, $J = 1.656\,917\,694\,08$ (left self-intersection, red curve, $n = 1$ in Table 1), $J = 1.036\,434\,991\,78$ (right self-intersection, red curve, $n = 2$ in Table 1) and neighbouring curves (blue and green lines).

5.2 Amplitude profiles with two singular points

It is possible, tuning the parameters properly, to obtain amplitude profile with two singular points.

Let, as before, $\kappa = 0.05$, $b = -0.001$, $a = 5$, $h = 0.5$, H being arbitrary. We can compute, for some H , from (26), (27) $X(H)$, $Y(H)$, then from Eqn. (28) we get $J_1(H)$ and $J_2(H)$ corresponding to two curves with one intersection each. The condition for a curve with two intersections is $J_1 = J_2$ for some H .

To find this value of H we compute J_1 , J_2 for two values of H , $H_0 = 0.40$, $H_1 = 0.55$, and use linear extrapolation to compute $H = H_{cr}$ such that $J_1(H_{cr}) = J_2(H_{cr})$. In one step of this procedure we compute new value of $H^{(i+2)}$ from known $H^{(i)}$, $J_1^{(i)}$, $J_2^{(i)}$ and $H^{(i+1)}$, $J_1^{(i+1)}$, $J_2^{(i+1)}$ solving linear system of equations for $\alpha^{(i,i+1)}$, $\beta^{(i,i+1)}$

$$\begin{aligned} J_1^{(i)} - J_2^{(i)} &= H^{(i)} \alpha^{(i,i+1)} + \beta^{(i,i+1)} \\ J_1^{(i+1)} - J_2^{(i+1)} &= H^{(i+1)} \alpha^{(i,i+1)} + \beta^{(i,i+1)} \end{aligned} \quad (29)$$

where $i = 0, 1, 2, \dots$. Then the next value of $H^{(i+2)}$ is computed as $H^{(i+2)} = -\frac{\beta^{(i,i+1)}}{\alpha^{(i,i+1)}}$. The convergence is quite fast, see Tables 2, 3.

Table 2				
$X_1^{(i)}$	$Y_1^{(i)}$	$J_1^{(i)}$	$H^{(i)}$	i
2.170 051 157	1.357 255 661	1.656 917 694	0.40	0
2.222 181 140	1.452 883 358	1.736 397 285	0.55	1
2.250 807 092	1.503 767 806	1.775 975 009	0.611 498 955	2
2.247 348 900	1.497 675 627	1.771 343 329	0.604 644 433	3
2.247 330 153	1.497 642 563	1.771 318 111	0.604 606 880	4
2.247 330 182	1.497 642 613	1.771 318 150	0.604 606 937	5

Table 3				
$X_2^{(i)}$	$Y_2^{(i)}$	$J_2^{(i)}$	$H^{(i)}$	i
4.835 083 103	4.192 055 014	1.036 434 992	0.40	0
4.793 018 228	2.753 798 647	1.555 975 411	0.55	1
4.620 272 267	2.513 582 261	1.798 606 879	0.611 498 955	2
4.641 565 672	2.538 879 342	1.771 466 643	0.604 644 433	3
4.641 680 711	2.539 018 448	1.771 317 923	0.604 606 880	4
4.641 680 536	2.539 018 236	1.771 318 150	0.604 606 937	5

Figures below show convergence of two curves with one singular point to one curve with two singular points.

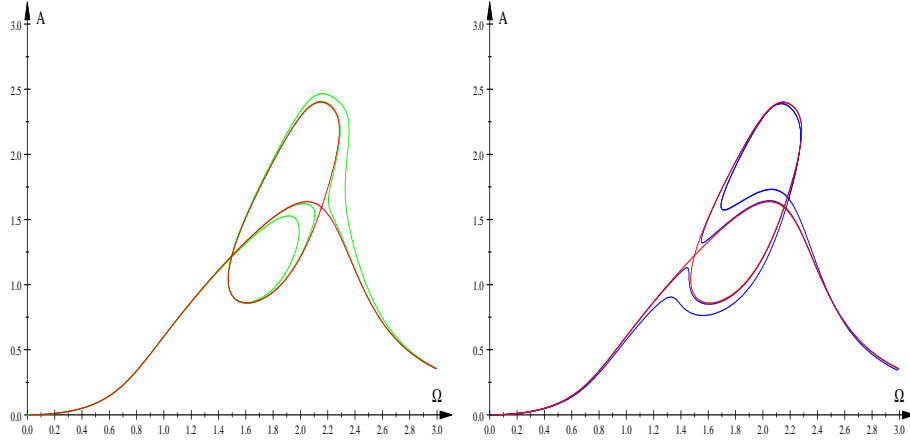


Figure 2: Convergence of amplitude profiles to critical amplitude profile with two singular points (red curve): convergence of curves from Table 2 (left figure, green curves), and from Table 3 (right figure, blue).

Bifurcation diagrams computed for parameters in the neighbourhood of such resonance curve display presence of two singular points, see Figs. 3.

In Figures 3 the parameters are $\kappa = 0.05$, $b = -0.001$, $a = 5$, $h = 0.5$ in both cases and $J = 1.745 481 261$, $H = 0.6054$ for Fig. 3a and $J = 1.740 481 261$, $H = 0.6034$ for Fig. 3b.

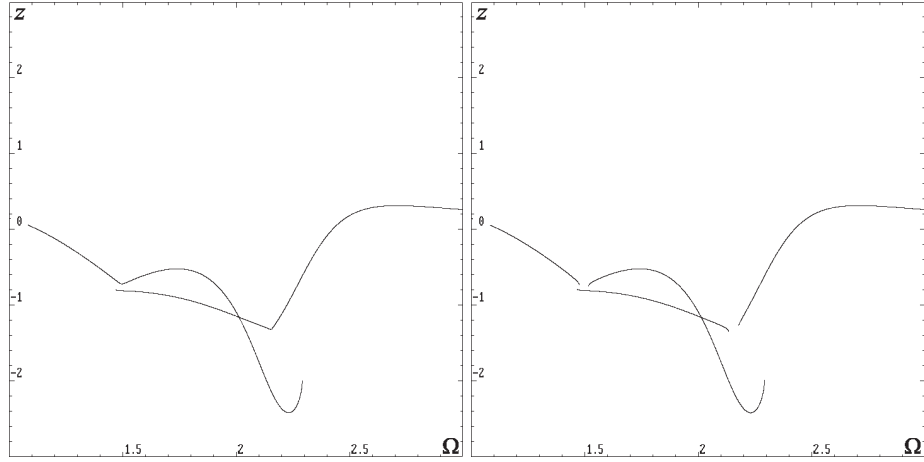


Figure 3: Bifurcation diagrams. The left figure corresponds the amplitude profile with singular point (left figure) with two cusps and to the nonsingular curve (right figure) with two gaps.

These diagrams correspond to amplitude profiles shown in Fig. 4.

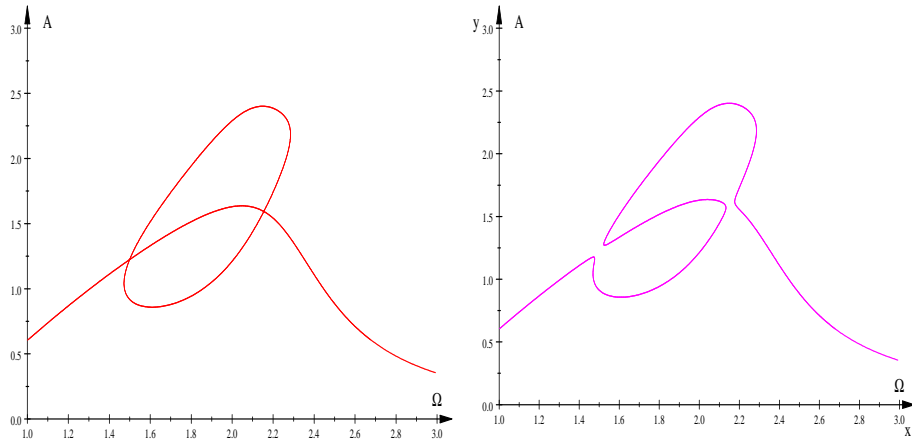


Figure 4: The amplitude profile with two singular points (left figure, red) and nonsingular curve (right figure, magenta).

5.3 Merging two singular points into a single degenerate point

It is possible, by smooth change of the parameters, to merge two singular points lying on the red curve in Figs. 2, 3. The resulting singular point is degenerate,

i.e. fulfills the following set of equations [16]:

$$\begin{aligned} L = 0, \quad \frac{\partial L}{\partial X} = 0, \quad \frac{\partial L}{\partial Y} = 0, \\ \frac{\partial^2 L}{\partial X^2} = 0, \quad \frac{\partial^2 L}{\partial X \partial Y} = 0, \quad \frac{\partial^2 L}{\partial Y^2} = 0, \end{aligned} \quad (30)$$

where $L(X, Y)$ is given by (23).

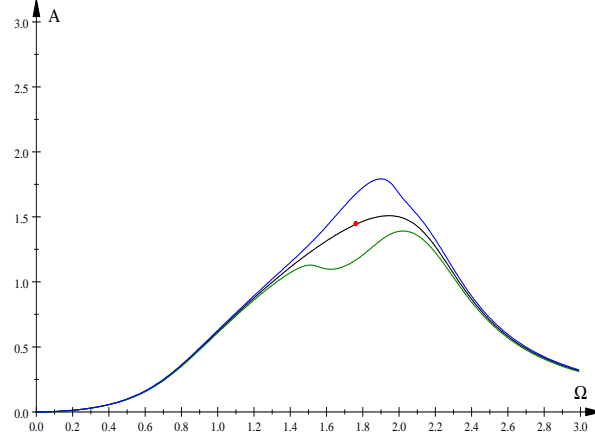


Figure 5: Amplitude profile with degenerate singular point (red dot) and two neighbouring curves.

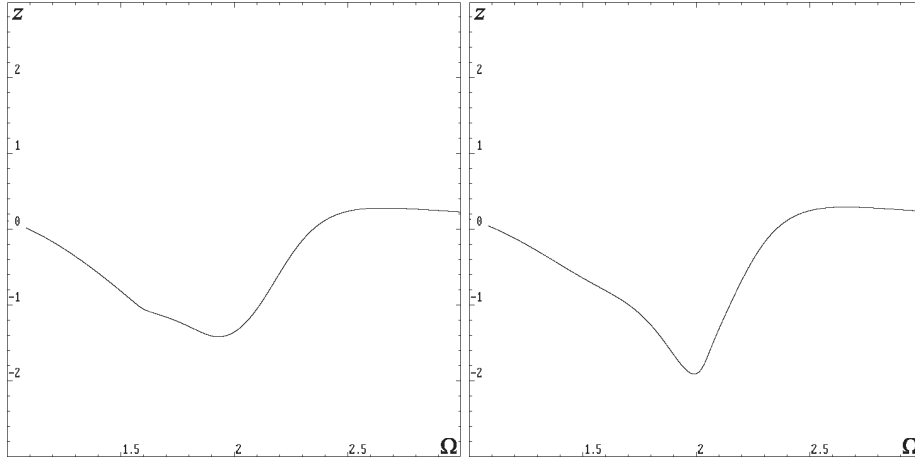


Figure 6: Metamorphosis of the bifurcation diagrams near amplitude profile with degenerate singular point.

Solving Eqns. (30) for $\kappa = 0.05$, $J = 1.771318150$ (these two parameters correspond to the parameters of the critical red curve with two singu-

lar points) we get $X = 3.113\,090\,974$, $Y = 2.087\,620\,813$, $h = 0.548\,982\,679$, $a = 4.538\,990\,962$, $b = -1.718\,542\,532 \times 10^{-2}$, $H = 0.644\,095\,068$, see Fig. 5.

Bifurcation diagrams computed in the neighbourhood of the degenerate singular point depend sensitively on small changes of parameters, Fig. 6.

6 Summary and discussion

In this work we have studied dynamics of two coupled periodically driven oscillators. The inner motion of this system has been described by the exact fourth-order equation (5) (or (10) in nondimensional form). Applying the KBM method we have computed approximate resonance curves (amplitude profiles) $A(\Omega)$. Although the KBM method is basically used for the second-order equations we managed to apply it to the fourth-order equation since it was possible to eliminate secular terms and impose steady-state conditions. Dependence of the amplitude A on the forcing frequency Ω is complex since $A(\Omega)$ is defined implicitly as an algebraic curve, $L(X, Y) = 0$, see Eqn.(23), with polynomial function L depending on variables $X = \Omega^2$, $Y = A^2$ and control parameters a , b , h , H , κ , J in a complicated manner.

In our previous paper we stressed that near singular points of algebraic curves, defining amplitude profiles, metamorphoses of bifurcation diagrams (and hence of dynamics) take place. In the present paper we have studied three cases of singular points of the resonance curves defined by Eqn.(23): i) the case of one singular point (Section 5.1), ii) the case of two singular points on one resonance curve (Section (5.2)), iii) the case of degenerate singular point (Section (5.3)). Indeed, dynamics of the system (10) changes significantly in the neighbourhood of singular points of resonance curve $L(X, Y) = 0$. Singular points described in Section 5 are just the tip of the iceberg and thus we are going to study multitude of singular points of amplitude profiles (23) in our future work.

References

- [1] J. P. Den Hartog, *Mechanical Vibrations* (4th edition), Dover Publications, New York 1985.
- [2] S. S. Oueini, A. H. Nayfeh and J.R. Pratt, Arch. Appl. Mech. **69**, 585 (1999).
- [3] W. Szemplińska-Stupnicka, *The Behavior of Non-linear Vibrating Systems*, Kluwer Academic Publishers, Dordrecht, 1990.
- [4] J. Awrejcewicz, *Bifurcation and Chaos in Coupled Oscillators*, World Scientific, New Jersey 1991.
- [5] J. Kozłowski, U. Parlitz and W. Lauterborn, Phys. Rev. E **51**, 1861 (1995).
- [6] K. Janicki, W. Szemplińska-Stupnicka, J. Sound. Vibr. **180**, 253 (1995).

- [7] A. P. Kuznetsov, N. V. Stankevich and L. V. Turukina, *Physica D* **238**, 1203 (2009).
- [8] J. Awrejcewicz, R. Starosta, *Theor. Appl. Mech. Lett.* **2**, 043002 (2012).
- [9] A. Okniński and J. Kyzioł, *Machine Dynamics Problems* **29**, 107 (2005).
- [10] A. Okniński and J. Kyzioł, *Differential Equations and Nonlinear Mechanics* **2006**, Article ID 56146 (2006).
- [11] J. Kyzioł and A. Okniński, *Acta Phys. Polon. B* **42**, 2063 (2011).
- [12] J. Kyzioł and A. Okniński, *Acta Phys. Polon. B* **43**, 1275 (2012).
- [13] J. Kyzioł and A. Okniński, *Differ. Equ. Dyn. Sys.*, DOI 10.1007/s12591-012-0132-8, published online: 04 July 2012.
- [14] R. Starosta, J. Awrejcewicz, L. Manevitch, in: *DYNAMICAL SYSTEMS. Analytical/Numerical Methods, Stability, Bifurcation and Chaos*, J. Awrejcewicz, M. Kaźmierczak, P. Olejnik, J. Mrozowski, Editors, The University of Łódź Publishing House, Łódź 2011; pp. 79–84.
- [15] A. H. Nayfeh, *Introduction to Perturbation Techniques*, John Wiley & Sons, New York 1981.
- [16] C. T. C. Wall, *Singular Points of Plane Curves*, Cambridge University Press, New York 2004.